

# Antiferromagnetic resonance and high magnetic field properties of $\text{NaNiO}_2$

 E. Chappel<sup>1,a</sup>, M.D. Núñez-Regueiro<sup>1</sup>, F. Dupont<sup>1</sup>, G. Chouteau<sup>1</sup>, C. Darie<sup>2</sup>, and A. Sulpice<sup>3</sup>
<sup>1</sup> Grenoble High Magnetic Field Laboratory, CNRS and MPI-FKF, BP 166X, 38042 Grenoble, France

<sup>2</sup> Laboratoire de Cristallographie, CNRS, BP 166X, 38042 Grenoble, France

<sup>3</sup> Centre de Recherches sur les Très Basses Températures, CNRS, BP 166X, 38042 Grenoble, France

Received 9 March 2000 and Received in final form 13 July 2000.

**Abstract.** Magnetisation measurements up to 23 T and submillimeter wave ESR in the frequency region 48–380 GHz have been performed on  $\text{NaNiO}_2$  powders at low temperature. Also typical spectra above the Néel temperature  $T_N$  are shown. At 4 K the magnetisation shows a spin-flop transition at 1.8 T and saturation at 10 T.  $M_S = 1\mu_B/\text{Ni}$  confirms the low spin state of the  $\text{Ni}^{3+}$  ions. The susceptibility exhibits a maximum at  $T_N = 20$  K with  $\mu_{\text{eff}} = 1.85\mu_B$  and  $\theta = +36$  K.  $\text{NaNiO}_2$  is an A-type antiferromagnet: we derive  $J_F = 13$  K and  $J_{AF} = -1$  K for the interactions between Ni ions within and between adjacent layers, respectively. The AFMR spectra yield an energy gap of 52.5 GHz, in agreement with the spin-flop value derived from the magnetisation. The anisotropy of the  $g$  factor observed at 100 K with  $g_{\perp} > g_{\parallel}$  can be attributed to the Jahn-Teller effect for  $\text{Ni}^{3+}$  ions in the low spin state, which stabilises the  $|3z^2 - r^2\rangle$  occupation. We finally comment on the isomorphic controversial  $\text{Li}_{1-x}\text{Ni}_{1+x}\text{O}_2$  compound.

**PACS.** 75.30.Et. Exchange and superexchange interactions – 76.50.+g Ferromagnetic, antiferromagnetic and ferrimagnetic resonances; spin-wave resonance

## 1 Introduction

The layered intercalation compounds are a subject of current research, due to their promising properties for batteries. They also show interesting structural and magnetic behaviours. For example, for  $\text{LiNiO}_2$  the realisation of a spin orbital liquid has been recently proposed, as a consequence of quantum fluctuations between eventually degenerate classical configurations [1], or simply due to the frustration of the triangular  $\text{Ni}^{3+}$  lattice preventing a staggered orbital ordering for the degenerate  $e_g$  states [2]. It is interesting to compare  $\text{LiNiO}_2$  with its isomorphic compound  $\text{NaNiO}_2$ , which exhibits long range magnetic order. In contrast with  $\text{LiNiO}_2$ , stoichiometric  $\text{NaNiO}_2$  can be synthesized, and it shows an antiferromagnetic stacking of triangular  $S = 1/2$  ferromagnetic planes. However, there has been only a few studies on this compound in the literature, after the synthesis by Dyer *et al.* in 1954 [3] and the pioneering work by Bongers and Enz in 1966 [4]: Kemp *et al.* [5] have measured (but not published) the magnetic susceptibility, Delmas *et al.* [6] have studied the effect of Co substitution on the Jahn-Teller (JT) distortion, and Dick. *et al.* [7] have determined the structure of the monoclinic phase.

Here a complete study of the static and dynamical magnetic properties of  $\text{NaNiO}_2$  is presented. The analysis of these results allows us to precise the values of the characteristic fields and of the intra- and inter-layer magnetic interactions.

## 2 Synthesis and structural characterization

Powder samples of  $\text{NaNiO}_2$  were prepared by reaction of 3.5 g of NiO and 2.62 g of  $\text{Na}_2\text{O}_2$  in an  $\text{Al}_2\text{O}_3$  crucible. Intimately ground mixture was heated under pure dry oxygen for 70 h at temperature of 700 °C, and then allowed to cool slowly to room temperature still under oxygen atmosphere. The resulting powder was a mixture of  $\text{NaNiO}_2$  with a small amount of NiO. Refiring this mixture with an excess of  $\text{Na}_2\text{O}_2$  (0.5 g) during 3 days with intermediate grinding led to pure samples of  $\text{NaNiO}_2$ .

$\text{NaNiO}_2$  crystallises at high temperature in the layered  $\alpha\text{-NaFeO}_2$  structure ( $R\bar{3}m$  space group) with a cubic close packed arrangement of the oxide ions. The lattice parameters in the hexagonal cell are:  $a = 2.96$  Å and  $c = 15.78$  Å. The layer sites, with octahedral coordination, are occupied alternatively by sodium ( $3a$  site) and nickel ( $3b$  site) ions.  $\text{NaNiO}_2$  undergoes a structural transition at 220 °C, attributed to the cooperative JT effect on the  $\text{Ni}^{3+}$  ions. The  $\text{NaNiO}_2$  low temperature phase

---

<sup>a</sup> e-mail: chappel@labs.polycnrs-gre.fr

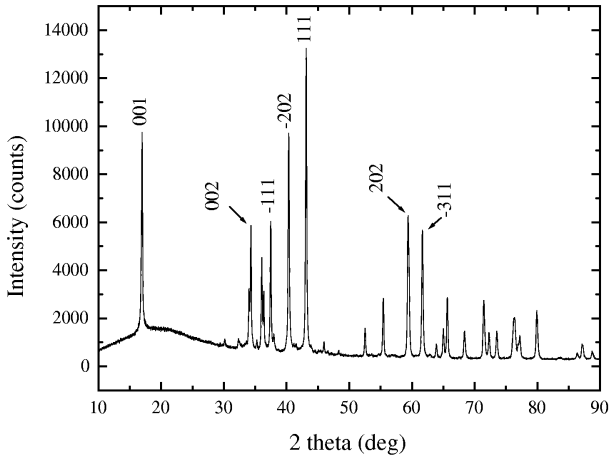


**Fig. 1.** X-ray powder diffraction pattern of  $\text{NaNiO}_2$  at room temperature.

is monoclinic, space group  $C_2^2$ , with lattice parameters:  $a = 5.318 \text{ \AA}$ ,  $b = 2.841 \text{ \AA}$ ,  $c = 5.574 \text{ \AA}$  and  $\beta = 110.485^\circ$ . The  $\text{NiO}_6$  octahedra are distorted (elongated) with 4 short and 2 long distances of  $1.904 \text{ \AA}$  and  $2.144 \text{ \AA}$ , respectively. X-ray powder patterns were collected for  $10^\circ \leq 2\theta \leq 90^\circ$  with a Siemens D5000 powder diffractometer in transmission mode, equipped with a Ge monochromator placed on the primary beam ( $\text{CuK}\alpha_1$  radiation,  $\lambda = 1.54056 \text{ \AA}$ ), a rotating sample and a mini PSD. The X-ray powder pattern shown in Figure 1 is in excellent agreement with the neutron scattering profile, showing the good quality of the sample.

### 3 Results

#### 3.1 Magnetic susceptibility and magnetisation

The magnetic susceptibility measurements were performed on a SQUID magnetometer under a 1 T field between 2 and 200 K using pressed pellets. The high magnetic field measurements (up to 23 T) were made at the Grenoble High Magnetic Field Laboratory facility using a Bitter magnet. The temperature dependence of  $H/M$  of  $\text{NaNiO}_2$  for  $H = 1 \text{ T}$  is reported in Figure 2. It can be fitted with a Curie-Weiss law between 200 and 100 K, with an effective moment of  $\mu_{\text{eff}} = 1.85\mu_B$  and  $\theta = +36 \text{ K}$ . The value of  $\mu_{\text{eff}}$  corresponds to the  $\text{Ni}^{3+}$  ion in the low spin state  $S = 1/2$  ( $t_{2g}^6 e_g^1$ ). Deviation from the paramagnetic linear regime is observed well above the Néel temperature  $T_N = 20 \text{ K}$ . This is the signature of short range order interactions often present in such quasi-2D systems.

The field dependence of the magnetization at 4 K up to 23 T is reported in Figure 3. Bongers and Enz [4] have found a spin-flop transition (*i.e.* the spins that had initially opposite direction to the applied field align perpendicular to it) at  $H_{\text{SF}} = 1.76 \text{ T}$  for a single crystal. We observe a change of slope in the  $M(H)$  curve around this value, as evidenced by the maximum of the susceptibility  $dM/dH$  plotted in the inset of Figure 3. Moreover,

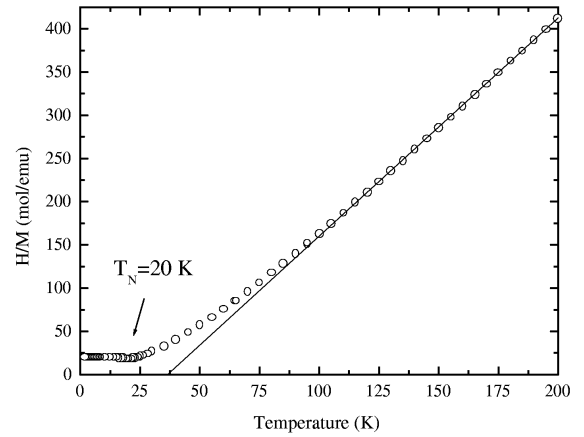


**Fig. 2.** Temperature dependence of  $H/M$  at  $H = 1 \text{ T}$  for  $\text{NaNiO}_2$ . The continuous line shows the Curie-Weiss law. The anomaly at the Néel temperature  $T_N$  is also indicated.

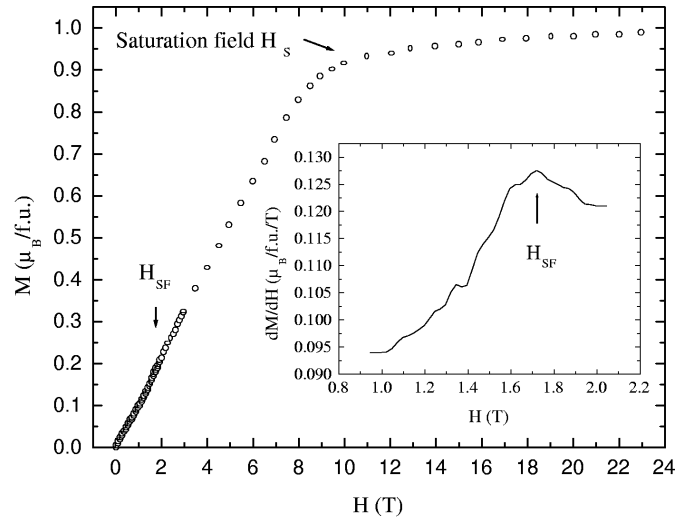


**Fig. 3.** Magnetic field dependence of the magnetisation at 4 K for layered  $\text{NaNiO}_2$ . The magnetic saturation is reached at  $H_S \approx 10 \text{ T}$ , with  $M_S = 1\mu_B/\text{Ni}$  as expected for  $\text{Ni}^{3+}$  in the low spin state  $S = 1/2$ . The inset shows the susceptibility around the spin-flop transition at  $H_{\text{SF}}$ .

for the first time, the saturation is reached, above 10 T, with a saturation moment  $M_S = 1\mu_B/\text{Ni}$ . This result is a good confirmation of the low spin state of the  $\text{Ni}^{3+}$  ion. We do not observe any spontaneous magnetisation or any hysteresis in the magnetisation curve at 4 K.

Figure 4 shows the temperature dependence of  $M/H$  under various magnetic fields around the spin-flop field  $H_{\text{SF}}$ . The most common method used to determine  $H_{\text{SF}}$  on a powder consists in measuring the field at which the ratio  $M/H$  does not decrease below  $T_N$  (see inset of Fig. 4). For  $H > H_{\text{SF}}$  and  $T < T_N$  the susceptibility is actually constant in a first approximation, since all spins are in a transverse configuration. We observe this transition at  $H_{\text{SF}} = (1.8 \pm 0.1) \text{ T}$ .

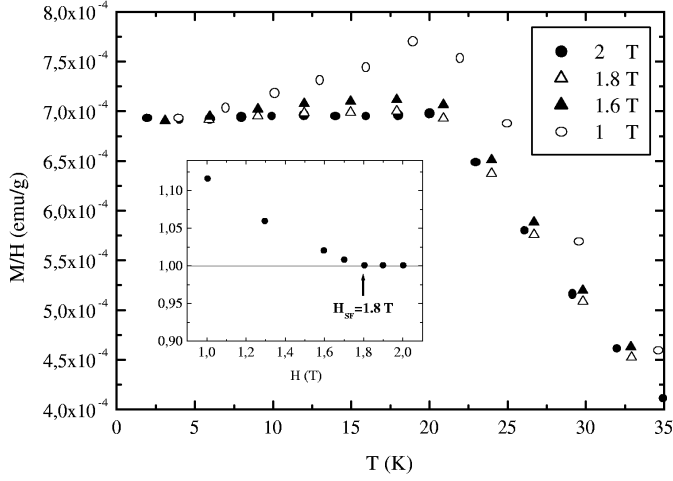


**Fig. 4.** Temperature dependence of  $M/H$  at different magnetic fields for NaNiO<sub>2</sub>. The field dependence of the ratio  $\frac{M/H(T=T_N)}{M/H(T=0)}$  is shown in the inset: the estimated spin-flop field is  $H_{SF} = 1.8$  T.

### 3.2 Dynamical study

Submillimeter electron spin resonance (ESR) measurements were carried out at different frequencies and temperatures, using Gunn oscillators and Carcinotrons. The magnetic field (up to 12 T) was produced by a superconducting magnet (Oxford).

A previous study [8] showed that in the paramagnetic regime the X-band electron paramagnetic resonance (EPR) signal is slightly asymmetric with a factor  $g_{\text{eff}} = 2.15$  at 100 K, and very broad. The signal narrows by decreasing the temperature until, just above  $T_N$ , it becomes again very broad and asymmetric as expected, while the resonance field drastically decreases. High frequency measurements at high temperatures ( $T > 100$  K) can be analysed in a JT approach of the Ni<sup>3+</sup> ion, with two anisotropic  $g$  factors. In fact, for a distorted octahedra the  $g$  tensor is axial (cylindrical symmetry). It is usual to define the trigonal axis as  $z$ ,  $g_z = g_{\parallel}$  and  $g_x = g_y = g_{\perp}$ . If the magnetic field makes an angle  $\theta$  with the trigonal axis  $z$ , the observed  $g$ -factor is:

$$g = (g_{\parallel}^2 \cos^2 \theta + g_{\perp}^2 \sin^2 \theta)^{1/2}. \quad (1)$$

The principal values of the  $g$ -tensor can be determined from a powder spectrum if the  $g$ -anisotropy is not too small. If there is no absorption at higher or lower fields than the principal values of the  $g$ -tensor, the onset of the absorption gives rise to sharp features in the derivative curve (see the spectrum at 100 K in Fig. 5). One finds  $g_{\parallel} < g_{\perp}$ , in agreement with an elongated octahedral environment for the Ni<sup>3+</sup> ions.

In Figure 5 we show our ESR study at 285 GHz at three selected temperatures above  $T_N$ . At 100 K the ESR spectrum looks anisotropic and the two features can be interpreted with  $g_{\parallel} = 1.967$  and  $g_{\perp} = 2.314$ . The positions of the lines do not change significantly between 300 and 100 K [8]. The first line, corresponding to  $g_{\perp}$  above

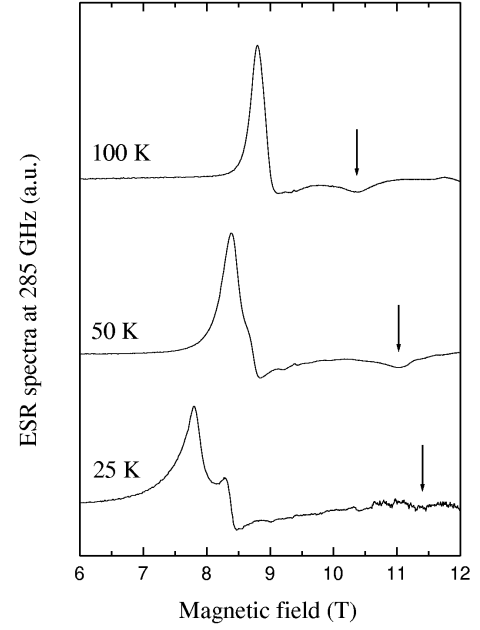


**Fig. 5.** High frequency ESR spectra of NaNiO<sub>2</sub> for three temperatures above the Néel temperature.

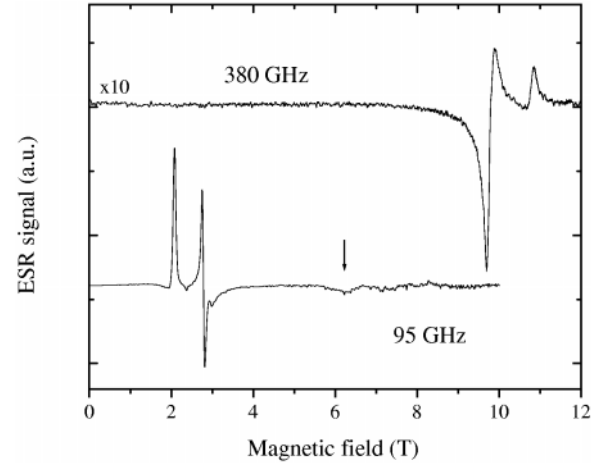


**Fig. 6.** ESR spectra of NaNiO<sub>2</sub> at  $T = 4$  K showing the inversion of the two (orthogonal) main lines with increasing frequency. The arrow indicates the parallel mode.

100 K, is shifted to lower fields with decreasing temperature, while the second feature (indicated by arrows) goes to higher fields. This splitting is certainly due to magnetic fluctuations since it is frequency dependent [8]. A new line appears at 50 K in the vicinity of the first peak, suggesting the presence of an anisotropy in the plane perpendicular to the trigonal axis. Figure 6 shows the ESR spectra of NaNiO<sub>2</sub> below the Néel temperature, taken at 95 and 380 GHz, which underline the inversion of these two orthogonal modes with increasing frequency.

This evolution of the ESR spectra allows us to plot the frequency-field diagram of Figure 7. The two crossing perpendicular modes seem to give rise to the same zero field gap of 52.5 GHz, as extrapolated from Figure 8.

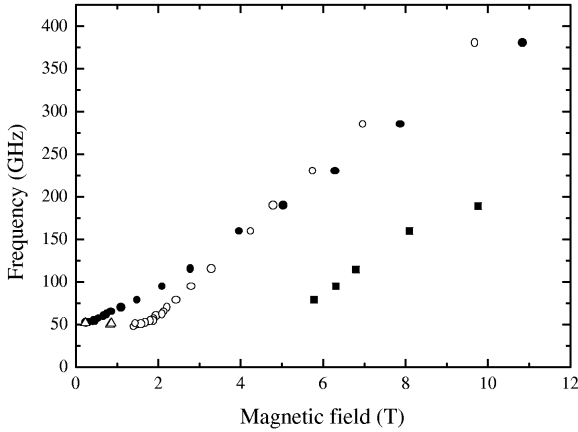


**Fig. 7.** AFMR frequency-field diagram of  $\text{NaNiO}_2$  at 4 K. The full and open circles correspond to the two orthogonal modes above the gap, while the triangles indicate the low frequency mode. The squares show the spin-flop mode.

## 4 Discussion

Let us discuss first the magnetic interactions expected in the  $\text{NaNiO}_2$  compound according to the Goodenough-Kanamori-Anderson (GKA) rules [9]. In the  $\text{NiO}_2$  slabs there are only  $90^\circ$  Ni-O-Ni bonds, while between slabs only  $180^\circ$  bonds take place via the oxygen ions. As it was shown before, the  $\text{Ni}^{3+}$  ions are in the low spin state ( $t_{2g}^6 e_g^1$ ). According to the Anderson approach, the interaction between two  $\text{Ni}^{3+}$  ions in adjacent Ni layers would be antiferromagnetic. In the case of semicovalency, the same result is expected since virtual excitations to the empty hybrid states ( $e_g sp_3$ ) involve the same full O  $2p$  orbitals. In contrast, for the  $90^\circ$  case, since virtual excitations occur from orthogonal O  $2p$  orbitals we cannot derive a conclusion for the sign of the magnetic interaction from the GKA rules. However, Hund's rule acting on the O ion will favour a ferromagnetic coupling between  $\text{Ni}^{3+}$  ions in the same layer.

Therefore, as proposed by Bongers and Enz [4], the magnetic structure of  $\text{NaNiO}_2$  can be described by a two sublattice model with ferromagnetic interactions within each Ni layer and antiferromagnetic interactions between adjacent Ni layers. Using the molecular field theory and taking  $H_E$  as the exchange field of sublattice 1 acting on sublattice 2, and  $H_A$  as the weak anisotropy field acting on one sublattice, the equations for the critical fields are:

$$\begin{cases} H_{\text{SF}} = [H_A(2H_E - H_A)]^{1/2} \\ H_S = 2H_E + H_A \end{cases} \quad (2)$$

where  $H_{\text{SF}}$  is the antiferromagnetic to spin-flop transition field and  $H_S$  the necessary field to achieve full saturation of the powder sample. These expressions are obtained by just writing the total energy of the system, *i.e.* the anisotropy, the exchange and the Zeeman terms, and then minimizing the energy as a function of the angle between the field and the sublattice magnetization [10]. From the experimental data we derive  $H_{\text{SF}} = (1.8 \pm 0.1)$  T (see Fig. 4) and  $H_S = (10 \pm 0.5)$  T (Fig. 3). This latter value was not

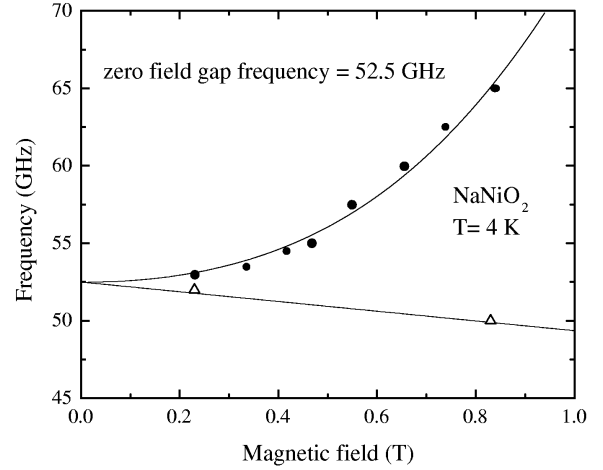


**Fig. 8.** Extrapolation of the AF gap from the low field data. The solid lines are just guides for the eyes.

previously measured. Solving the set of equations (2), we find  $H_E = (4.8 \pm 0.1)$  T and  $H_A = (0.35 \pm 0.1)$  T. These values are in agreement with those of reference [4] except a factor 2 in their formula that we do not understand. Since the  $t_{2g}$  orbitals are full, the real orbital moment is quenched and we do not expect significant spin-orbit coupling. The origin of the magnetic anisotropy must be the dipolar interaction, rather small for  $S = 1/2$ , as observed. In the layered  $\text{LiFeO}_2$  compound the  $\text{Fe}^{3+}$  ions are in the high spin state ( $^6S$ ) and consequently there is no spin-orbit coupling. The dipolar coupling is proportional to  $\mu^2/r^3$  and since the distance between transition metal ions (TM) of  $\text{NaNiO}_2$  and  $\text{LiFeO}_2$  [11] are not very different, we can compare their anisotropy fields:  $H_A(\text{LiFeO}_2)/H_A(\text{NaNiO}_2) \approx \mu(\text{Fe}^{3+})^2/\mu(\text{Ni}^{3+})^2$ . We observe an experimental value of 9 instead of 25. In fact, we just expect the same order of magnitude as the dipolar field is very sensitive to the TM-TM distance.

Now we are able to derive the values of the magnetic couplings. Each  $\text{Ni}^{3+}$  ion has 6 nearest neighbours in the same layer and 3 near neighbours in each of the two adjacent layers. The interlayer exchange interaction can be expressed as  $J_{\text{AF}}$  for a pair of  $\text{Ni}^{3+}$  ions [12]:

$$E_{\text{Exchange}} = -2J_{\text{AF}}\mathbf{S}_1\mathbf{S}_2 \quad (3)$$

and  $J_{\text{AF}}$  can be determined from  $H_E$ :

$$g\mu_B H_E = 12J_{\text{AF}}S \quad (4)$$

where  $g$  is the gyromagnetic factor,  $\mu_B$  the Bohr magneton and  $k_B$  the Boltzmann factor. We obtain:

$$J_{\text{AF}}/k_B = (-1 \pm 0.1) \text{ K}. \quad (5)$$

This small value is not surprising since the exchange mechanism involves two O ions. In fact, Goodenough predicts for the Ni-O-O-Ni bond an interaction at least one order of magnitude smaller than for Ni-O-Ni [13]. The low spin state of the Ni ion with  $S = 1/2$  has been unambiguously confirmed by the high field measurements since the magnetisation reaches the value  $M_S/\text{Ni} = 1\mu_B$ , as discussed

before. On the other hand, the total magnetisation  $M_{\text{tot}}$  in the high temperature limit can be written:

$$M_{\text{tot}} = g\mu_B \langle S_{\text{tot}} \rangle = \frac{C}{T - \theta} \quad (6)$$

where  $C$  is the Curie constant and  $\theta$  the Weiss temperature:

$$k_B\theta = \frac{2}{3}S(S+1)[6(J_F + J_{AF})]. \quad (7)$$

With the parameters derived before, this expression gives us the intraplane ferromagnetic interaction between Ni<sup>3+</sup> ions,  $J_F = +13$  K. This value seems more realistic than  $J_F = 32$  K obtained in reference [4], as it is well known that 90° interactions are generally weak. On the other hand,  $J_F \approx 10$  K was obtained for the equivalent intraplane Ni<sup>3+</sup>-O-Ni<sup>3+</sup> interaction in the isomorphous Li<sub>1-x</sub>Ni<sub>1+x</sub>O<sub>2</sub> compound [14].

An expression for the Néel temperature can be obtained by assuming that at  $T_N$  a spontaneous magnetisation occurs in absence of an applied magnetic field. This gives:

$$k_B T_N = \frac{2}{3}S(S+1)[6(J_F - J_{AF})]. \quad (8)$$

Replacing in equation (8) the values obtained before yields  $T_N = +40$  K, twice the experimental value defined at the maximum of  $M/H(T)$ , showing the important role of short range interactions in the vicinity of  $T_N$ . The departure from the Curie-Weiss law well above  $T_N$  for all samples is the signature of this effect, *i.e.* the molecular field model cannot give a good value of  $T_N$  for systems with important short range correlations. NaNiO<sub>2</sub> is in fact a quasi two-dimensional system since the magnetic Ni layers are well isolated by the diamagnetic Na layers, as evidenced by the large ratio between the intra- and the inter-layer magnetic interactions  $J_F/J_{AF}$ .

In order to discuss the spectra of Figure 7 we show in Figure 9 the theoretical AFMR modes for the simplest model: an uniaxial antiferromagnetic single crystal at  $T = 0$  K, given by equations (9–12) (see Ref. [15]). For  $H_{\parallel}$  and  $H < H_{\text{SF}}$ :

$$\frac{\omega}{\gamma} = \sqrt{2H_A H_E + H_A^2 + \left(\frac{\alpha H}{2}\right)^2} \pm H \left(1 - \frac{\alpha}{2}\right) \quad (9)$$

with  $\alpha = \chi_{\parallel}/\chi_{\perp}$ , where  $\chi_{\parallel}$  ( $\chi_{\perp}$ ) is the parallel (perpendicular) susceptibility. For  $H_{\parallel}$  and  $H > H_{\text{SF}}$ :

$$\frac{\omega}{\gamma} = \sqrt{\frac{1}{2}H^2 - 2H_A H_E + H_A^2 + (H_E - H_A) \frac{H^2}{2H_E}}. \quad (10)$$

The corresponding equations for  $H_{\perp}$  are:

$$\frac{\omega}{\gamma} = \sqrt{\frac{1}{2}H^2 + 2H_A H_E + H_A^2 + (H_E + H_A) \frac{H^2}{2H_E}} \quad (11)$$

$$\frac{\omega}{\gamma} = \sqrt{2H_A H_E + H_A^2 - H_A \frac{H^2}{2H_E}}. \quad (12)$$

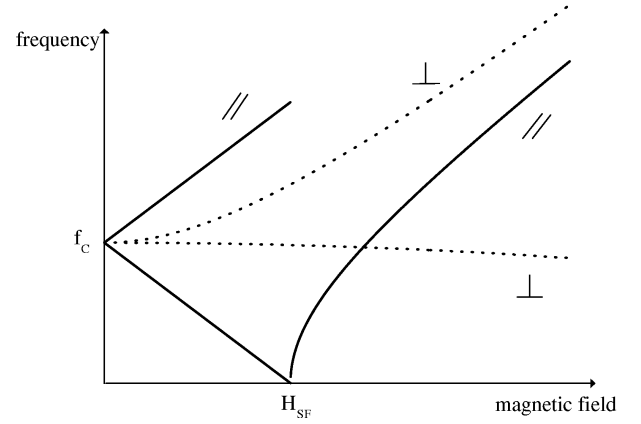


**Fig. 9.** Theoretical AFMR frequency-field diagram for an uniaxial antiferromagnetic single crystal with  $\alpha = \chi_{\parallel}/\chi_{\perp} = 0$ . We call  $f_c$  the zero field gap frequency and  $H_{\text{SF}}$  the spin-flop field. In a powder all crystallite orientations are present and we observe a broad AFMR spectrum, as explained in the text.

In a powder all crystallite orientations are present and we observe in the AFMR spectra only broad lines around the single crystal modes. As can be seen in Figure 5, and even better in Figure 6, in our case the perpendicular mode is splitted. However, the frequency dependence of these two lines seems to converge to the same zero field gap, as shown in Figure 7. Replacing the values of  $H_E = 4.8$  T and  $H_A = 0.35$  T obtained before in equation (9), we find a zero field gap frequency of  $f_c = 52.5$  GHz, in good agreement with the value of 52.5 GHz, extrapolated from Figure 8. In this figure the slightly decreasing line under the gap should correspond to the mode given by equation (12), in which the last term  $H_A H^2/2H_E$  cannot be neglected. The spin-flop mode, indicated by an arrow in Figure 6 and given by equation (10), can be added in the frequency-field diagram of Figure 7. With decreasing temperature this parallel mode goes towards the high field region while the perpendicular one shifts to lower fields. As we have said before, we believe that this effect has magnetic origin since it is frequency dependent. One can correlate this behaviour with the deviation from the paramagnetic linear regime of the susceptibility observed well above  $T_N$  in Figure 2. These features are both signatures of an internal ferromagnetic field.

We have recently done measurements on Li<sub>1-x</sub>Ni<sub>1+x</sub>O<sub>2</sub>. We have found that with decreasing  $x$  ( $x \leq 0.01$ ), the high field magnetisation approaches the curve of NaNiO<sub>2</sub> [17]. However the stoichiometric compound cannot be synthesized. An old mystery remains without definite explanation: why Li<sub>1-x</sub>Ni<sub>1+x</sub>O<sub>2</sub> does not show macroscopic JT effect? It has been proposed that the pure system would resemble the NaNiO<sub>2</sub> compound but the presence of some Ni ions in the Li layers induces magnetic frustration, preventing the magnetic ordering [14,17]. Armstrong *et al.* [18] notice that the replacement of Mn<sup>3+</sup> by Co<sup>3+</sup> in LiMnO<sub>2</sub> results in a shortening of the (Mn/Co-O) bond approaching Ni-O in Li<sub>1-x</sub>Ni<sub>1+x</sub>O<sub>2</sub>. They propose that the absence of cooperative JT effect in Li<sub>x</sub>Mn<sub>1-y</sub>Co<sub>y</sub>O<sub>2</sub> and Li<sub>1-x</sub>Ni<sub>1+x</sub>O<sub>2</sub>

may have a similar origin, keeping in mind that very small transition metal vacancies are able to destroy the orbital ordering. Recently the absence of spin and orbital ordering in  $\text{Li}_{1-x}\text{Ni}_{1+x}\text{O}_2$  has been also interpreted as the realisation of an orbital-spin liquid state: since the Li oxide is more 3 dimensional than the Na oxide, it is argued that strong orbital fluctuations will suppress any ordering [1]. In order to test the validity of these arguments, experiments on  $\text{NaNiO}_2$  under pressure are in progress.

## 5 Conclusions

We report in this paper a complete magnetic study of  $\text{NaNiO}_2$  at low temperatures. At 4 K, we observe a metamagnetic transition at  $H_{\text{SF}} = 1.8$  T and the saturation at  $H_{\text{S}} = 10$  T. The magnetic structure of  $\text{NaNiO}_2$  below  $T_{\text{N}} = 20$  K corresponds to an A-type antiferromagnet, with ferromagnetic coupling  $J_{\text{F}} = +13$  K within the Ni layers and antiferromagnetic coupling  $J_{\text{AF}} = -1$  K between adjacent Ni layers. The quasi-two dimensional character of this system induces magnetic fluctuations up to temperatures well above  $T_{\text{N}}$ , as it has been discussed in the different static and dynamical measurements.

The AFMR spectra are observed, with an energy gap of 52.5 GHz, in good agreement with the values of the characteristic fields derived from static measurements. At  $T = 100$  K two anisotropic  $g$  factors are measured:  $g_{\perp} = 2.314$  and  $g_{\parallel} = 1.967$ . Their ratio confirms the occupation of the  $|3z^2 - r^2\rangle$  state, *i.e.* a ferrodistorive orbital ordering.

The knowledge of the magnetic properties of  $\text{NaNiO}_2$  can now be used as reference to study the behaviour of other isomorphic compounds. Experiments on  $\text{NaNiO}_2$  under pressure should help to elucidate

the controversial ground state of quasi-stoichiometric  $\text{Li}_{1-x}\text{Ni}_{1+x}\text{O}_2$ .

We gratefully acknowledge P. Rabu and S. de Brion for useful discussions.

## References

1. L.F. Feiner, A.M. Oles, J. Zaanen, Phys. Rev. Lett. **78**, 2799 (1997); Phys. Rev. B **61**, 6257 (2000).
2. Y. Kitaoka *et al.*, J. Phys. Soc. Jpn **67**, 3703 (1998).
3. L.D. Dyer, B.S. Borie, G.P. Smith, J. Am. Chem. Soc. **76**, 1499 (1954).
4. P.F. Bongers, U. Enz, Solid State Comm. **4**, 153 (1966).
5. J.P. Kemp, P.A. Cox, J.W. Hodby, J. Phys. Cond. Matt. **2**, 6699 (1990).
6. C. Delmas, I. Saadoun, P. Dordor, Mol. Cryst. Liq. Cryst. **244**, 337 (1994).
7. S. Dick, M. Müller, F. Preissinger, T. Zeiske, Powder Diffraction **12**, 239 (1997).
8. E. Chappel *et al.*, Eur. Phys. J. B **17**, 615 (2000).
9. D.I. Khomskii, G.A. Sawatsky, Solid State Comm. **102**, 87 (1997).
10. A. Herpin, *Théorie du Magnétisme* (Presses Universitaires de France, Paris, 1968), p. 495.
11. E. Chappel, G. Chouteau, M. Holzapfel, A. Ott (preprint).
12. P.W. Anderson, Solid State Phys. **14**, 99 (1963).
13. J.B. Goodenough, *Magnetism and the chemical bond* (Interscience-Wiley, New-York, 1963).
14. M.D. Núñez-Regueiro, E. Chappel, G. Chouteau, C. Delmas, Eur. Phys. J. B **16**, 37 (2000).
15. S. Foner, in Rado Suhl, *Magnetism I* (Academic Press, 1963), p. 383.
16. R. Lacroix, U. Höchli, K.A. Müller, Helv. Phys. Acta **37**, 627 (1964).
17. E. Chappel (to be published).
18. A.R. Armstrong, A.D. Robertson, R. Gitzendanner, P.G. Bruce, J. Solid State Chem. **145**, 549 (1999).